Available online at www.sciencedirect.com
ScienceDirect
Ceramics International 37 (2011) 753–758
CERAMICS INTERNATIONAL
www.elsevier.com/locate/ceramint

Effect of solvent on structure and optical properties of PZT nanoparticles prepared by sol–gel method, in infrared region

A. Khorsand Zak [a,b,*], W.H. Abd. Majid [a]

[a] Low Dimensional Materials Research Center, Department of Physics, University of Malaya, Kuala Lumpur 50603, Malaysia
[b] Material and Electroceramics Lab., Department of Physics, Ferdowsi University of Mashhad, Mashhad 91775-1436, Iran

Received 28 May 2010; received in revised form 28 July 2010; accepted 3 October 2010
Available online 17 November 2010

Abstract

Single-phase perovskite $Pb(Zr_{0.52},Ti_{0.48})$ nanoparticles, PZT-NPs were prepared by the sol–gel method with two different solvents, 2-methoxyethanol, EGME, and poly ethylene glycol, PEG. X-ray diffraction (XRD) was used to study of the structure of the PZT-NPs. Fourier transform infrared spectroscopy (FTIR) was used to measure the infrared reflectivity spectrum in the range of 4000–280 cm^{-1}. Infrared active vibration modes of BO_6 octahedral (ν_1 and ν_2) were observed for PZT-NPs below 600 cm^{-1}. The third vibration mode of Pb against the TiO_3 group, ν_3, occurred below the experimentally accessible range. The Kramers–Kronig method (K–K) and classical dispersion theory were applied to analyze the data and calculation of the optical constants such as reflective index ($N(\omega)$)and permittivity ($\varepsilon(\omega)$). The results showed that the structure and optical properties of PZT-NPs were changed by different type of solvent.

Keywords: C. Optical properties; D. PZT; Nanoparticle; Permittivity

1. Introduction

The study of dielectric resonance is becoming an important theme in the physics of composites, and has fascinated physicists for many decades due to its numerous applications in photonic crystals (PCs) [1]. Further miniaturization and large-scale integration of these systems are limited by apparent finite size effects, which diminish the dielectric response [2]. One of these materials is lead zirconate titanate $Pb(Zr_x,Ti_{1-x})O_3$, PZT, which exhibits pyroelectric, piezoelectric and electro-optical properties. This material is promising for practical applications such as infrared detectors, ferroelectric non-volatile random access memories [3], optical modulators and optical waveguides [4]. Synthesizing the single phase of PZT nanoparticles, PZT-NPs, which are free of the pyrocholore phase, for these applications is the main task of researchers seeking to prepare a good device for these applications. Fourier transform infrared data analysis has long been known as a good way to study the optical properties of materials. One method that can be used to analysis the IR data is the Kramers–Kronig (K–K) mathematical method. K–K is an appropriate method that can be used to analyze the IR reflectance spectra of various materials, from organic to inorganic, solid to liquid and single crystal, polycrystalline and amorphous [5–7]. FTIR spectroscopy is widely used for material characterization [8–12]. Although many papers have reported the synthesis of PZT-NPs, the optical properties of perovskite PZT-NPs however, have rarely been investigated. It is known that the preparation processes are critical in modifying the properties of the sol–gel nanoparticles and ceramics [13–15]. Many factors, such as solvents, dopants and modifiers, are often decisive. The choice of solvent can affected phase development [16], morphology [17], particle size [18] and optical properties [19,20].

In this work, we used 2-methoxyethanol and poly ethylene glycol as different solvents to prepare PZT-NPs by the sol–gel method. The optical properties of PZT-NPs, namely the reflectance, phase evolution, refractive index, extinction coefficient, real and imaginary part of dielectric constant and loss energy function were investigated by the K–K relations.

* Corresponding author at: Low Dimensional Materials Research Center, Department of Physics, University of Malaya, Kuala Lumpur 50603, Malaysia. Tel.: +60 12 2850849, fax: +60 37 9674146.
E-mail address: alikhorsandzak@gmail.com (A.K. Zak).

0272-8842/$36.00
doi:10.1016/j.ceramint.2010.10.020

2. Experimental

$Pb(Zr_{0.52},Ti_{0.48})O_3$ nanoparticles, PZT-NPs, were derived from a soft chemical process. Lead acetate trihydrate ($Pb(CH_3COO)_2{\cdot}3H_2O$, Merck), titanium isopropoxide ($Ti(OCH(CH_3)_2)_4$, Merck), zirconium n-propoxide ($Zr(OCH_2CH_2CH_3)_4$, and 70% in 1-propanol, Sigma–Aldrich), 2-methoxyethanol and poly ethylene glycol were used as two different solvents to prepare the precursor solutions for PZT-NP drawing. The atomic ratio of the Pb:Zr:Ti of the solution was 1:0.52:0.48 and 10% excess lead acetate was introduced. Details of the preparation method can be found in the literature [21,22]. The polymeric precursor solutions were dried and calcinated at two different temperatures of 600 and 650 °C, to achieve pure perovskite PZT-NPs. X-ray diffraction analysis was used to study the formation of the perovskite phase in the range of 15–80° by Cu Kα radiation. The FTIR results were used to calculate the absorption and reflectance parameters at range of 4000–280 cm^{-1}. The K–K method was used to analyze the reflection spectra to obtain the optical parameters of PZT-NPs.

3. Results and discussion

3.1. X-ray diffraction analysis

The X-ray diffraction pattern of PZT-NPs prepared with two different solvents, 2-methoxyethanol, PZT–EGME and poly ethylene glycol, PZT–PGE, by the sol–gel method, are shown in Fig. 1. For PZT–EGME, Fig. 1a, the rhombohedral phase was observed for both heating treatments, and the perovskite phase is clearly formed at these temperatures. A perovskite structure is also for PZT–PGE, Fig. 1b, but a tetragonal phase was achieved by using poly ethylene glycol as the solvent for the sol–gel process. A small amount of pyrocholore phase was found at a calcination temperature of 600 °C for both methods. The pyrocholore phase disappeared and a pure perovskite structure was obtained when the calcination temperature was increased to 650 °C.

The typical TEM image of the PZT-NPs prepared in different solvents are shown in Fig. 2. From TEM analysis the primary particle size of the powders can be determined. The primary particles size of the PZT-NPs prepared in PEG and EGME were found to be approximately 25 and 17 nm, respectively.

3.2. FTIR analysis

The room temperature transmittance of PZT-NPs has been investigated by Fourier Transform Infrared spectroscopy (FTIR) in the range of 280–4000 cm^{-1}. The spectra are shown in Fig. 3. A broad band was observed for each spectrum, with minimum transmittance at 530 cm^{-1}, and another band was observed with minimum transmittance at 350 cm^{-1}. From the previous studies, these two absorption bands were attributed to TiO_6 and ZrO_6 stretching and bending in the octahedral normal modes. In the perovskite PZT structure, one Ti\Zr ion was bonded to six oxygen ions. A vertical axis was considered,

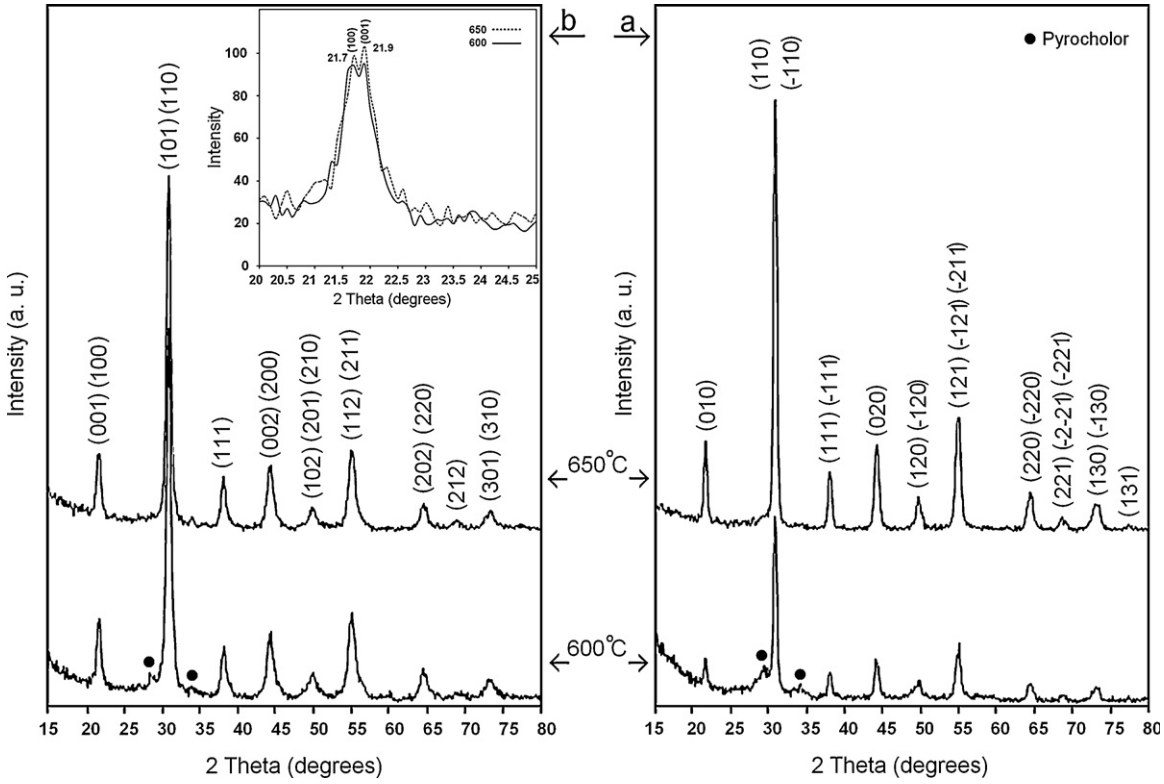

Fig. 1. X-ray diffraction pattern of PZT–EGME (a) and PZT–PEG (b) calcined at 600 °C and 650 °C. Pure perovskite structure was obtained at 650 °C. Also the first XRD peak of PZT–PEG clearly shows a tetragonal phase.

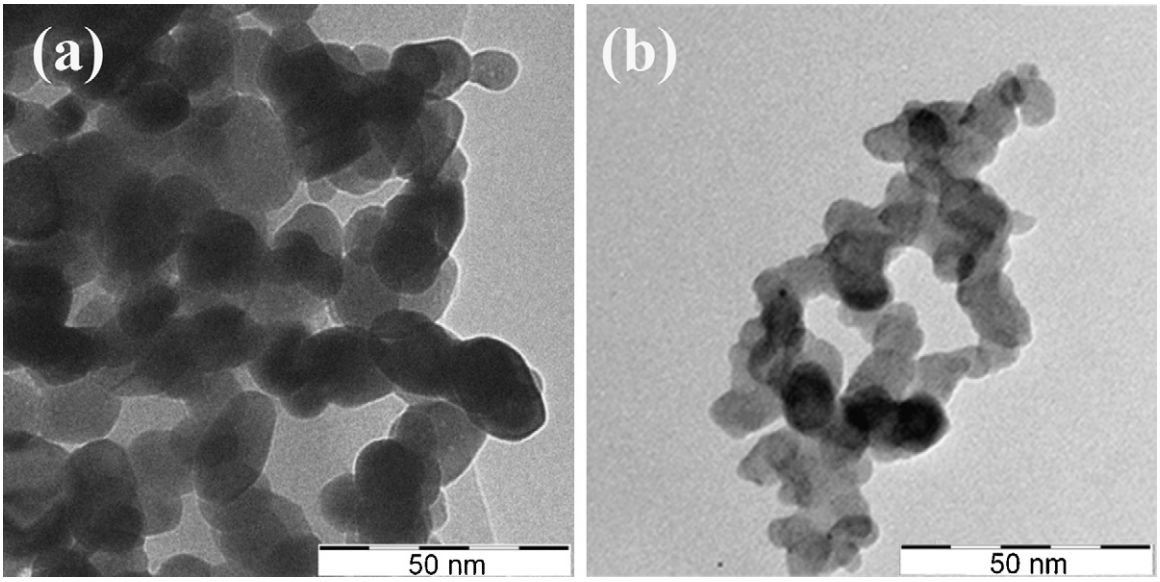

Fig. 2. TEM morphology of the PZT-NPs prepared in different solvent media. (a) PZT–PEG and (b) PZT–EGME.

connecting one Ti\Zr ion to two oxygens, as shown in Fig. 4. The stretching vibration is the motion of Ti\Zr and O that changes the length of the Ti\Zr–O_1 bond, as in Fig. 4a. The bending vibration occurs when there is a change in the O_1–Ti\Zr–O_2 bond angle, as shown in Fig. 4b. The higher frequency band, ν_1, is assigned to the stretching normal vibration, and the lower band, ν_2, is assigned to the bending normal vibration [23]. There were few changes in the transmittance trace for the composites prepared by different solvents. Two small bands are also observed around 1500 and 3500 cm^{-1} in both of the PZT–PEG FTIR traces, which can be attributed to O–H and C–H bands from the remained burned organic materials. The FTIR results showed the formation of the perovskite structure of PZT-NPs, and they were in good agreement with the XRD results described previously [24]. There is another vibration mode (ν_3), which was described as a vibration of the cation-TiO_3\ZrO_3 bond but this vibration mode is below the available experimental frequency range (280–4000 cm^{-1}) used in this research [25]. The results were presented in Table 1.

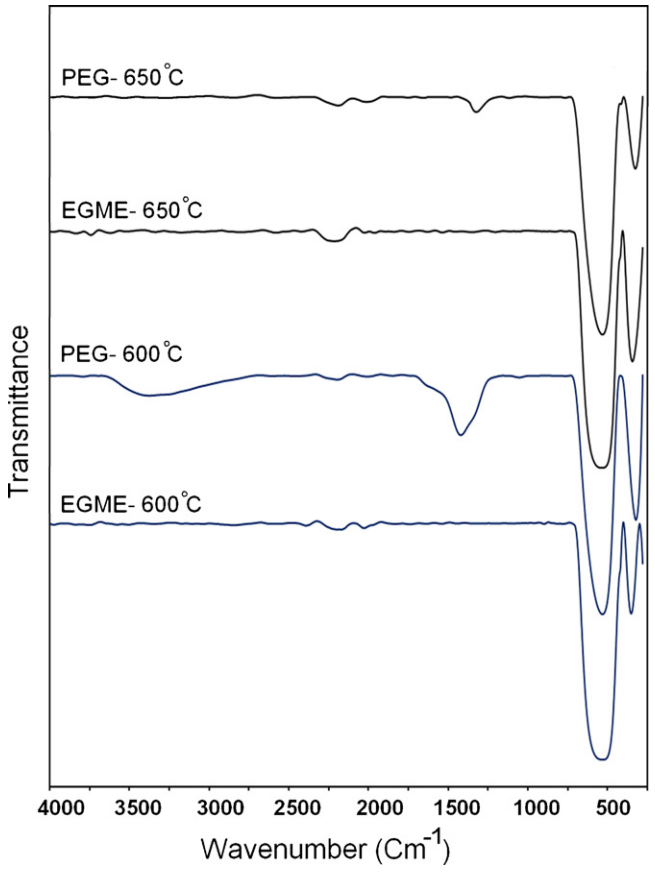

Fig. 3. FTIR pattern of PZT–EGME and PZT–PEG calcined at 600 °C and 650 °C. The two important bands those are related to perovskite structure are seen in all FTIR traces.

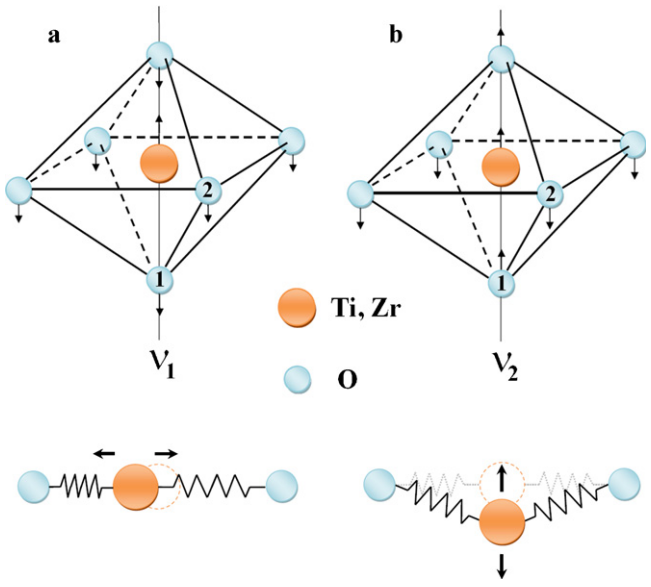

Fig. 4. Schematic infrared active normal vibrations of a TiO_6 octahedron, ν_1, higher frequency stretching vibration, ν_2, lower frequency bending vibration.

Table 1
Vibration bands and band widths for PZT–EGME and PZT–PEG calcined at 600 °C and 650 °C.

Material	Temperature (°C)	ν_1 (cm^{-1})	Band wide ν_1(cm^{-1})	ν_2 (cm^{-1})	Band wide ν_2 (cm^{-1})
PZT–EGME	650	530	340	352	98
PZT–PEG	650	532	336	326	148

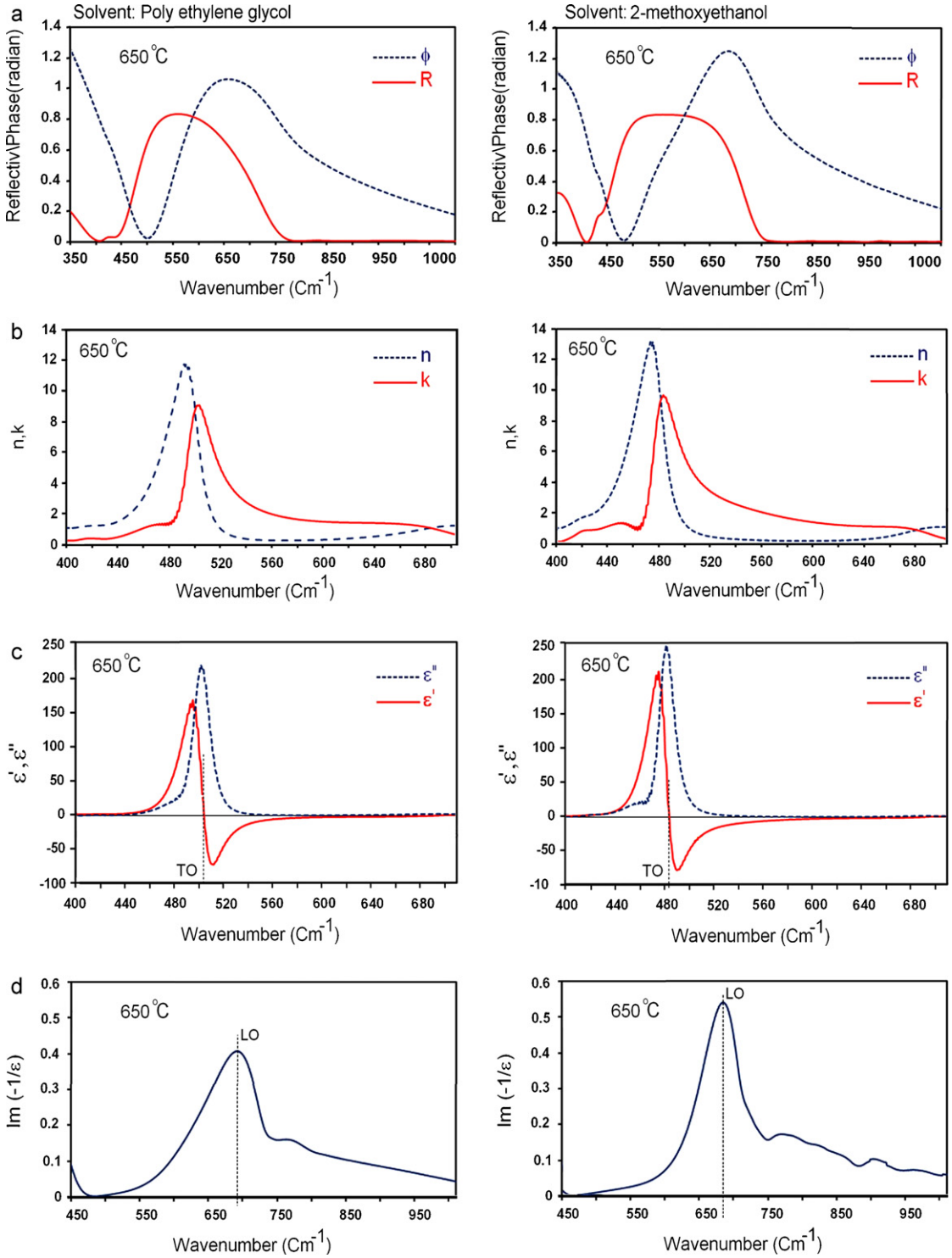

Fig. 5. The reflectance and phase change spectrum, (a) refractive index and extinction coefficient, (b) real and imaginary parts of dielectric functions, (c) and electron-energy-loss function, (d) of PZT–EGME and PZT–PEG calcined at 650 °C.

4. Evaluation of the optical constants

4.1. Theory of K–K method

The K–K method was used to evaluate the optical constant of PZT-NPs prepared by the sol–gel method using FTIR transmittance spectra data. Absorption is characterized by a decrease in transmitted light intensity through the sample. The quantity used to discuss absorption as a function wavenumber is the transmittance (T), which is the ratio of the intensity of the light transmitted through the sample (I) to the initial light intensity (I_0). The transmittance is related to the more common percent transmittance ($T\%$) by $T\% = 100T$. The absorption (A) is defined as $\log_{10}(1/T)$, according to Lambert's principle [26].

$$A(\omega) = \log\frac{I_0}{I} = \log_{10}\frac{1}{T(\omega)} = \mathrm{Z} - \log_{10}(T(\omega)\%) \tag{1}$$

$$\Rightarrow R(\omega) = 100 - [T(\omega) + A(\omega)] \tag{2}$$

where $R(\omega)$ is the reflectance in the particular wavenumber. The reflective index N is the most widely used physical quantity in optical design. It is generally a complex quantity:

$$\tilde{N}(\omega) = \eta(\omega) + ik(\omega) \tag{3}$$

where $n(\omega)$ is the real part and $k(\omega)$ is the imaginary part of a complex reflective index. These constants can be calculated by the following equation:

$$\eta(\omega) = \frac{1 - R(\omega)}{1 + R(\omega) - 2\sqrt{R(\omega)}\cos\varphi(\omega)} \tag{4}$$

$$k(\omega) = \frac{2\sqrt{R(\omega)}\sin\varphi(\omega)}{1 + R(\omega) - Z\sqrt{R(\omega)}\cos\varphi(\omega)} \tag{5}$$

where $R(\omega)$ is the reflectance and $\varphi(\omega)$ is the phase change between the incidence and the reflected signal at a particular wave number ω. This phase change can be obtained from the K–K dispersion relation [27].

$$\varphi(\omega) = \frac{-\omega}{\pi}\int_0^{\infty}\frac{\ln R(\omega') - \ln R(\omega)}{\omega^{sz} - \omega^{z}}\,d\omega' \tag{6}$$

where $R(\omega)$ is the reflectance and $\varphi(\omega)$ is the phase change between the incidence and the reflected signal at a particular wave number ω. $\varphi(\omega)$ is obtained from Fourier transform of K–K dispersion relation [28].

$$\varphi(\omega_j) = \frac{4\omega_j}{\pi} \times \Delta\omega \times \sum_t \frac{\ln\left(\sqrt{R(\omega)}\right)}{\omega_t^2 - \omega_j^2} \tag{7}$$

where $\Delta\omega = \omega_{i+1} - \omega_i$ and if the data interval j is an odd number then $i = 2, 4, 6, \ldots, j-1, j+1, \ldots$ while if j is an even number then $i = 1, 3, 5, \ldots, j-1, j+1, \ldots$.

The dielectric function is the square of the refractive index. Consequently, the real and imaginary parts of the complex dielectric function can be written as follows:

$$\bar{\varepsilon}(\omega) = [\tilde{N}(\omega)]^2 = [n(\omega) + ik(\omega)]^2 \tag{8}$$

$$\Rightarrow \varepsilon'(\omega) + i\varepsilon''(\omega) = n^2(\omega) - k^2(\omega) + 2in(\omega)k(\omega) \tag{9}$$

$$\Rightarrow \begin{cases} \varepsilon'(\omega) = n^2(\omega) - k^2(\omega) \\ \varepsilon''(\omega) = 2n(\omega)k(\omega) \end{cases} \tag{10}$$

4.2. Optical constants spectrum

The optical constant spectrums of the PZT-NPs prepared by the two different solvents, calcinated at 650 °C, are shown in Fig. 5. As shown in Fig. 5a, the value of R and φ depend on the choice of solvent. It is observed that a broad reflection peak exists for PZT–EGME. The refractive index, n, and extinction coefficient, k, from 400 cm^{-1} to 700 cm^{-1}, are shown in Fig. 5b. Although the n and k peaks are shifted to higher wavenumbers for PZT–PEG compared with PZT–EGME, the values of the n and k peaks increase for PZT–EGME. The real and imaginary parts of the dielectric function of PZT-NPs are shown in Fig. 5c, and the main area of ε' and ε'' is from 400 cm^{-1} to 600 cm^{-1}. The ε' and ε'' peak positions of PZT–EGME are shifted to lower wavenumbers with increased values compared to those of PZT–PEG.

It seems that when the solvent is changed in the sol–gel process, the chemical reactions are changed and the lattice parameters and phases are affected by these changes. On the other hand, the resonance vibration frequencies of atom chains are related to the lattice parameters, so by changing the solvent, the optical parameters should also be changed.

4.3. Optical phonon modes

The optical longitudinal, LO, and transverse optical, TO, phonons are useful to describe the optical interactions with the lattice. The TO mode frequencies correspond to the peaks of the imaginary part of the dielectric function $\varepsilon(\omega)$, and the LO mode frequencies are obtained from the imaginary part of $1/\varepsilon$, as in Fig. 5d. Moreover, the TO and LO optical modes can be obtained from the reflection and extinction traces, respectively. There are two intersection points for the n and k graphs. As shown in Fig. 5b, the first point, with the lower wavenumber, is related to TO, and the second point, with the higher wavenumber, is related to the LO mode [29]. The transverse and longitudinal optical phonons of PZT-NPs are presented in Table 2.

Table 2
Optical phonon for PZT–EGME and PZT–PEG calcined at 600 °C and 650 °C.

	Material	Temperature (°C)
		650
Transverse optical phonon (TO), cm^{-1}	PZT–EGME	478
	PZT–PEG	496
Longitudinal optical phonon (LO), cm^{-1}	PZT–EGME	683
	PZT–PEG	693

5. Conclusions

We have reported a combined experimental and theoretical study of the optical properties of PZT nanoparticles. The PZT-NPs were synthesized by the sol–gel method using 2-methoxyethanol and poly ethylene glycol as two different solvents. The XRD patterns indicate the perovskite structure for both PZT–EGME and PZT–PEG. The optical properties of the PZT-NPs were investigated by transmittance measurements in the range of 280–4000 cm^{-1} and two bands were observed from the FTIR graphs. The broad band in the transmittance curve is a composition of the ν_1-TiO_3 and ν_1-ZrO_3 stretching normal vibration modes. The Kramers–Kronig method was used to evaluate the optical constants of PZT-NPs. The results showed that the optical constants of PZT-NPs depend on the solvent type that is used in the sol–gel preparation process.

Acknowledgments

This work was supported by University of Malaya through grants no: PS217\2009A and University Malaya HIRGA J-00000-73583. Authors are acknowledging Mr. Majid Darroudi for his constructive helps.

References

[1] P. Halevi, A.A. Krokin, J. Arriaga, Photonic crystals as optical components, Appl. Phys. Lett. 75 (1999) 2725–2727.
[2] L.M. Fraser, W.M.C. Foulkes, G. Rajagopal, R.J. Needs, S.D. Kenny, A.J. Williamson, Finite-size effects and Coulomb interactions in quantum Monte Carlo calculations for homogeneous systems with periodic boundary conditions, Phys. Rev. B 53 (1996) 1814–1832.
[3] Y.J. Seo, J.S. Park, W.S. Lee, Chemical mechanical polishing of PZT thin films for FRAM applications, Microelectronic Eng. 83 (2006) 2238–2242.
[4] L. Poffo, P.L. Auger, P. Benech, P. Benech, Determination of refractive index variation of a glass-integrated optical waveguide by the acousto-optic effect, Meas. Sci. Technol. 20 (2009), 45303 (5 pp.).
[5] M.E. Mezeme, S. Lasquellec, C. Brosseau, Dielectric resonances at optical frequencies using metal nanoshells, J. Phys. D: Appl. Phys. 42 (2009) 135420.
[6] O. Bazkir, Determination of optical constants of silicon photodiode from reflectivity measurements at normal incidence of light, Opt. Laser Eng. 45 (2007) 245–248.
[7] L.N. Latyev, V.Ya. Chekhovskoi, E.N. Shestakov, Determining the optical constants of metals by the Kramers–Kronig method, Appl. Spectrosc. 45 (1986) 1114–1117.
[8] A.E. Lavat, C.C. Wagner, J.E. Tasca, Interaction of Co–ZnO pigments with ceramic frits: A combined study by XRD, FTIR and UV–visible, Ceram. Inter. 34 (2008) 2147–2153.
[9] K. Singh, I. Bala, V. Kumar, Structural, optical and bioactive properties of calcium borosilicate glasses, Ceram. Inter. 35 (2009) 3401–3406.
[10] N. Qin, X.C. Fan, S.Y. Wu, X.M. Chen, Infrared reflection spectra of $Ba_{6-3x}Sm_{8+2x}Ti_{18}O_{54}$ ($x = 0.5$, 0. 67, and 0. 75) microwave dielectric ceramics, J. Appl. Phys. 101 (2007) 64103–64109.
[11] V. Zelezny, D. Chvostova, I. Szafraniak, M. Alexed, D. Hesse, Characterization of PZT nanostructures by infrared spectroscopy, J. Eur. Ceram. Soc. 27 (2007) 4321–4323.
[12] M. Rode, A. Borgschulte, A. Jacob, C. Stellmach, U. Barkow, J. Schoenes, Evidence for ionic bonding in YH_{32}d, Phys. Rev. Lett. 87 (2001) 235502 (4pp).
[13] M. Zhang, I.M.M. Salvado, P.M. Vilarinho, Synthesis and characterization of lead zirconate titanate fibers prepared by the sol–gel method: the role of the acid, J. Am. Ceram. Soc. 89 (2003) 775–785.
[14] M. Ghasemifard, S.M. Hosseini, A. Khorsand Zak, Gh.H. Khorrami, Microstructural and optical characterization of PZT nanopowder prepared at low temperature, Phys. E 41 (2009) 418–422.
[15] G. Mu, S. Yang, J. Li, M. Gua, Synthesis of PZT nanocrystalline powder by a modified sol–gel process using water as primary solvent source, J. Mater. Process. Technol. 182 (2007) 382–386.
[16] T.I. Chang, S.C. Wang, C.P. Liu, C.F. Lin, J.L. Huang, Thermal behaviors and phase evolution of lead zirconate titanate prepared by sol–gel processing: the role of the pyrolysis time before calcination, J. Am. Ceram. Soc. 91 (2008) 2545–2552.
[17] G. Hare'l, B.G. Ravi, R. Chaim, Effects of solvent and agitation on microstructural characteristics of sol–gel derived nanocrystalline Y-TZP powders, Mater. Lett. 39 (1999) 63–76.
[18] K.G. Kanade, B.B. Kale, R.C. Aiyer, B.K. Das, Effect of solvents on the synthesis of nano-size zinc oxide and its properties, Mater. Res. Bull. 41 (2006) 590–600.
[19] M. Durmus, T. Nyokong, Synthesis and solvent effects on the electronic absorption and fluorescence spectral properties of substituted zinc phthalocyanines, Polyhedron 26 (2007) 2767–2776.
[20] J.P. Zhang, S.Y. Zhou, P. Chen, O. Tsuneki, H. Masaaki, The effect of solvent on the optical properties of cyanine dye films, Dyes Pigm. 51 (2001) 93–101.
[21] A. Khorsand Zak, W.H.Abd. Majid, Characterization and X-ray peak broadening analysis in PZT nanoparticles prepared by modified sol–gel method, Ceram. Inter. 36 (2010) 1905–1910.
[22] Z.D. Qing, W.S. Jun, S.H. Shan, W.X. Li, C.M. Sheng, Synthesis and mechanism research of an ethylene glycol-based sol–gel method for preparing PZT nanopowders, J. Sol–Gel Sci. Technol. 41 (2007) 157–161.
[23] W.G. Spitzer, R.C. Miller, D.A. Kleinman, L.E. Howarth, Far infrared dielectric dispersion in $BaTiO_3$, $SrTiO_3$ and TiO_2, Phys. Rev. 126 (1962) 1710–1721.
[24] J.T. Last, Infrared-absorption studies on barium titanate and related materials, Phys. Rev. 105 (1957) 1740–1750.
[25] C.H. Perry, B.N. Khanna, Infrared studies of perovskite titanates, Phys. Rev. 135 (1964) A408–A412.
[26] D.C. Harris, M.D. Bertolucci, Symmetry, Spectroscopy and Introduction to Vibrational Electronic Spectroscopy, Dover, New York, 1978.
[27] V. Lucarini, J.J. Saarinen, K.E. Peiponen, E.M. Vartiainen, Kramers–Kronig Relations in Optical Materials Research, Springer, Berlin/Heidelberg/New York, 2004.
[28] M. Ghasemifard, S.M. Hosseini, Gh.H. Khorrami, Synthesis and structure of PMN–PT ceramic nanopowder free from pyrochlore phase, Ceram. Int. 35 (2009) 2899–2905.
[29] S.S. Ng, Z. Hassan, H. Abu Hassan, Kramers–Kronig analysis of infrared reflectance spectra with a single resonance, J. Teknol. 44 (2006) 67–76.